Coupling Efficiency of Butt-Joined Isotropic and Anisotropic Single-Mode Slab Waveguides

Shinnosuke Sawa, *Member, IEEE,* Masahiro Geshiro, *Member, IEEE,* Masashi Hotta, and Haruo Kanetake

Abstract—**Studied is the effect of axial displacement and angular misalignment on power-coupling efficiency of a butt-joint between an isotropic and an anisotropic single-mode slab waveguide. The power-coupling coefficient is formulated by means of the boundary conditions at the interface of the butt-joint and the orthogonality relations between the modes in the outgoing waveguide. It is found from the numerical results that proper amounts of angular misalignment and axial displacement remarkably suppress transmission losses when the material coordinate system of the anisotropic waveguide is not aligned with its waveguide coordinate system in the plane defined by the propagation axis and the normal of waveguide surface.**

I. Introduction

LOSS reduction in power coupling between two waveguides has been one of the most important problems in light transmission optics. Butt-joining is a simple method widely used in connecting waveguides different in structure. Coupling efficiency with this method critically depends on both axial placement and angular alignment. Up to now a lot of practical junctions have been investigated theoretically and experimentally: fiber splices [1]–[5], coupling from light sources into fibers or channel-waveguides [6]–[8], coupling between fibers and/or channel-waveguides [9]–[11], etc.

Most optical components and integrated circuits have been fabricated on anisotropic crystalline materials. Higher coupling efficiency in butt-joints between fibers and channel waveguides will be increasingly required for future use of pigtailed optical devices in practical applications. To the authors' knowledge, however, there are few studies on butt-joints between fibers and channel waveguides consisting of anisotropic materials; no work has been reported which includes misalignment between the waveguide and material coordinate systems in the anisotropic waveguide. The angle between both coordinate axes is called oblique angle hereafter. Only Marcuse has predicted that an appropriate amount of angular misalignment between two waveguide axes would increase the power coupled under such a situation [12].

Manuscript received April 4, 1991; revised October 1, 1991.

S. Sawa is with the Electrical Engineering Department, University of Osaka Prefecture, 4-808, Mozu-Umemachi, Sakai, Osaka, 591, Japan.

M. Geshiro, M. Hotta, and H. Kanetake are with the Department of Electronics Engineering, Ehime University, Bunkyo-3, Matsuyama, Ehime, 790, Japan.

IEEE Log Number 9104764.

In the present paper, power-coupling efficiency is estimated for a butt-joint between an isotropic slab waveguide and an anisotropic one consisting of uniaxial crystalline material which has the optical axis in an arbitrary direction in the plane defined by the propagation axis and the normal of waveguide surface. Uncoupled TE and TM modes can be supported in slab waveguides with such oblique angles. We concentrate on analyzing the characteristics of TM modes because of their interesting behavior which cannot be observed in isotropic waveguides. Usually the power-coupling characteristics of more practical butt-joints between fibers and channel waveguides can be estimated almost directly from those for slab waveguides which are much simpler in structure and analysis.

II. Waveguiding Structure

An incoming isotropic slab waveguide (waveguide 1) with thickness d_1 is butt-jointed to an outgoing anisotropic slab waveguide (waveguide 2) with thickness d_2 as shown together with the coordinate systems used for the analysis in Fig. 1. The waveguide 1 is assumed to be symmetric. The waveguide 2 may be either symmetric or asymmetric. It is also assumed that only the dominant mode can be supported by each of these waveguides. Optical waves propagate along the z' axis in the waveguide 1 and along the z axis in the waveguide 2. Δ is a displacement distance along the x axis and θ a misalignment angle, in the x-z plane, between the z and z' axes. In the following, subscripts 1 and 2 will be attached to the quantities belonging to the waveguides 1 and 2, respectively. ϵ_{1p} and $\hat{\epsilon}_{2p}$ whose additional subscript p, signifying the region, represents c (core) or d (cladding) are the scalar permittivity and the tensor permittivity, respectively. ϵ_0 is the free-space permittivity.

Suppose optical axes, in both core and cladding of the waveguide 2, are contained in the x-z plane and are parallel to each other. In the waveguide coordinate system, the permittivity tensor is then expressed as

$$\hat{\epsilon}_{2p} = \begin{pmatrix} \epsilon_{xxp} & 0 & \epsilon_{xzp} \\ 0 & \epsilon_{yyp} & 0 \\ \epsilon_{xzp} & 0 & \epsilon_{zzp} \end{pmatrix} \tag{1}$$

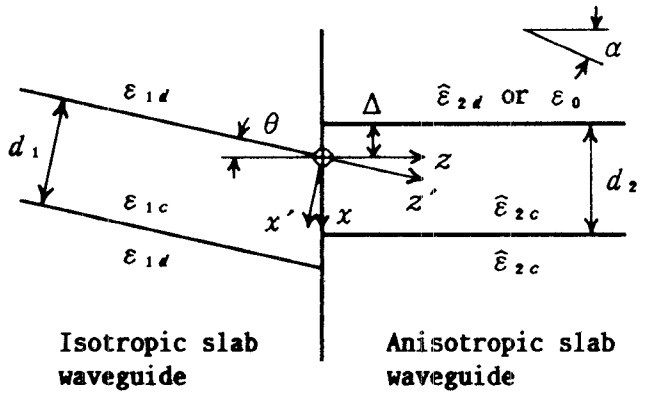

Fig. 1. Waveguide butt-joint and coordinate systems for the analysis.

where

$$\epsilon_{xxp} = \epsilon_{op} \cos^2 \alpha + \epsilon_{ep} \sin^2 \alpha$$
$$\epsilon_{xzp} = (\epsilon_{ep} - \epsilon_{op}) \sin \alpha \cos \alpha$$
$$\epsilon_{zzp} = \epsilon_{op} \sin^2 \alpha + \epsilon_{ep} \cos^2 \alpha$$
$$\epsilon_{yyp} = \epsilon_{op}. \tag{2}$$

In the above equations, ϵ_{op} and ϵ_{ep} are the permittivities for the ordinary and extraordinary rays, respectively. α is the oblique angle between the z axis and the optical axis. In general, angular misalignment makes a wedge-shaped air gap at the end-to-end junction. This gap, however, would be filled up with an index-matching liquid. Therefore, the butt-joint shown in Fig. 1 can be considered a good approximation to a practical butt-joint.

III. Analytical Method

We concentrate our discussion on the TM mode propagation as mentioned before. In the case of the dominant mode incidence, we obtain

$$H_y^{(i)} + rH_y^{(r)} + \int_0^\infty r(\rho_1)\, H_y^{(r)}(\rho_1)\, d\rho_1 = tH_y^{(t)} + \int_0^\infty t(\rho_2)\, H_y^{(t)}(\rho_2)\, d\rho_2 \tag{3}$$

$$E_x^{(i)} + rE_x^{(r)} + \int_0^\infty r(\rho_1)\, E_x^{(r)}(\rho_1)\, d\rho_1 = tE_x^{(t)} + \int_0^\infty t(\rho_2)\, E_x^{(t)}(\rho_2)\, d\rho_2 \tag{4}$$

from the boundary conditions at the joint, $z = 0$. In the above equations, the time variation factor $\exp(j\omega t)$ is suppressed. The superscripts (i), (r), and (t) are added to the incident, reflected, and transmitted waves, respectively. E_x is the x component of the electric field and H_y the y component of the magnetic field. The quantities represented as functions of ρ_1 or ρ_2, the propagation constants in the transverse direction, belong to radiation modes and r, t, $r(\rho_1)$, and $t(\rho_2)$ are unknown amplitude coefficients.

When $\theta \neq 0$, we can express the field components tangential to the $z = 0$ plane in the waveguide 1 in terms of the field components described with the (x', y', z') coordinate system as follows:

$$H_y^{(i)} = H_{y'}^{(i)} \tag{5}$$
$$H_y^{(r)} = H_{y'}^{(r)} \tag{6}$$
$$E_x^{(i)} = E_{x'}^{(i)} \cos\theta + E_{z'}^{(i)} \sin\theta \tag{7}$$
$$E_x^{(r)} = E_{x'}^{(r)} \cos\theta + E_{z'}^{(r)} \sin\theta \tag{8}$$

where the mathematical description for the field components in the right-hand sides is summarized in Appendix I.

Usually, the refractive indices of two waveguides do not differ much for most fiber-to-channel butt-joints: about 1.5 in usual fibers consisting of fused silica and 2.27 or 2.2 in channel-waveguides made of $LiNbO_3$, the most common anisotropic bulk material used for optical devices. The interface of these two materials would reflect at most 4% of the incident power of plane wave for the normal incidence; less for incident TM waves tilted up to the Brewster angle. Judging from this fact, we can omit reflected radiation modes in (3) and (4) without causing any significant errors. After multiplying these equations by the complex conjugate of $H_y^{(t)}$, we integrate the resulting equations with respect to x over the infinite region. The orthogonality relations between the modes in the waveguide 2 finally lead to

$$\int \frac{1}{\epsilon_{xx}} H_y^{(i)} H_y^{(t)*}\, dx + r \int \frac{1}{\epsilon_{xx}} H_y^{(r)} H_y^{(t)*}\, dx = t \int \frac{1}{\epsilon_{xx}} |H_y^{(t)}|^2\, dx \tag{9}$$

$$\int E_x^{(i)} H_y^{(t)*}\, dx + r \int E_x^{(r)} H_y^{(t)*}\, dx = t \int E_x^{(t)} H_y^{(t)*}\, dx \tag{10}$$

where the asterisk indicates the complex conjugate. Expressing E_x in H_y with the help of Maxwell's equations and applying the weakly-guiding approximation, we obtain

$$t = \frac{\frac{1}{\epsilon_{1d}}\left[\int h_1 H_y^{(t)*}\, dx \int H_y^{(r)} H_y^{(t)*}\, dx - \int H_y^{(t)} H_y^{(t)*}\, dx \int h_2 H_y^{(t)*}\, dx\right]}{\left[\frac{\epsilon_{xzd}}{\eta_d} \int H_y^{(r)} H_y^{(t)*}\, dx \int h_3 H_y^{(t)*}\, dx + \beta_2 \frac{\epsilon_{zzd}}{\eta_d} \int H_y^{(r)} H_y^{(t)*}\, dx \int |H_y^{(t)}|^2\, dx - \frac{1}{\epsilon_{1d}} \int h_2 H_y^{(t)*}\, dx \int |H_y^{(t)}|^2\, dx\right]} \tag{11}$$

where

$$\eta_d = \epsilon_{xxd}\epsilon_{zzd} - \epsilon_{xzd}^2. \tag{12}$$

In the above equations, β_1 and β_2 are the propagation constants of the dominant mode and h_1, h_2, and h_3 are given in Appendix II.

We here define the power-coupling coefficient through the joint as the ratio of the power of the transmitted dominant mode to the power of the incident mode, that is,

$$T = |t|^2 \frac{\dfrac{\beta_2}{\epsilon_{xxd}} \displaystyle\int |H_y^{(t)}|^2\, dx}{\dfrac{\beta_1}{\epsilon_{1d}} \displaystyle\int |H_{y'}^{(i)}|^2\, dx'}. \tag{13}$$

IV. Results of Calculations

We will present here some numerical results for two typical cases. The outgoing waveguide, which is assumed to be consisting of $LiNbO_3$, is symmetric in the first and is asymmetric in the second. The refractive indices of the incoming waveguide are chosen so that $n_{1c} = (\epsilon_{1c}/\epsilon_0)^{1/2} = 1.51275$ and $n_{1d} = (\epsilon_{1d}/\epsilon_0)^{1/2} = 1.51$. These are representative values for optical fibers in practical use. The slab thickness is assumed as $d_1 = d_2 = 5\lambda_0$ in both incoming and outgoing waveguides where λ_0 is a free space wavelength. In the case that the outgoing waveguide has a graded index profile, a multi-layer approximation is applied to the modal analysis [13].

A. Symmetric Index Profile

Index profiles, whether graded or not, would be almost symmetric in waveguides buried in the deep inside of substrates by means of special fabrication processes. Consider two typical symmetric index profiles in the waveguide 2. The first is a step index profile expressed as

$$n_o(x) = \begin{cases} n_{od}, & x < 0 \\ n_{od} + \delta n_o, & 0 \leqq x \leqq d_2 \\ n_{od}, & d_2 < x \end{cases}$$

$$n_e(x) = \begin{cases} n_{ed}, & x < 0 \\ n_{ed} + \delta n_e, & 0 \leqq x \leqq d_2 \\ n_{ed}, & d_2 < x. \end{cases} \tag{14}$$

The second is a square-law index profile described as

$$n_o(x) = \begin{cases} n_{od}, & x \leqq 0 \\ n_{od} + \delta n_o \left[1 - \left(\dfrac{x - d_2/2}{d_2/2}\right)^2\right], & 0 \leqq x \leqq d_2 \\ n_{od}, & d_2 \leqq x \end{cases}$$

$$n_e(x) = \begin{cases} n_{ed}, & x < 0 \\ n_{ed} + \delta n_e \left[1 - \left(\dfrac{x - d_2/2}{d_2/2}\right)^2\right], & 0 \leqq x \leqq d_2 \\ n_{ed}, & d_2 < x. \end{cases} \tag{15}$$

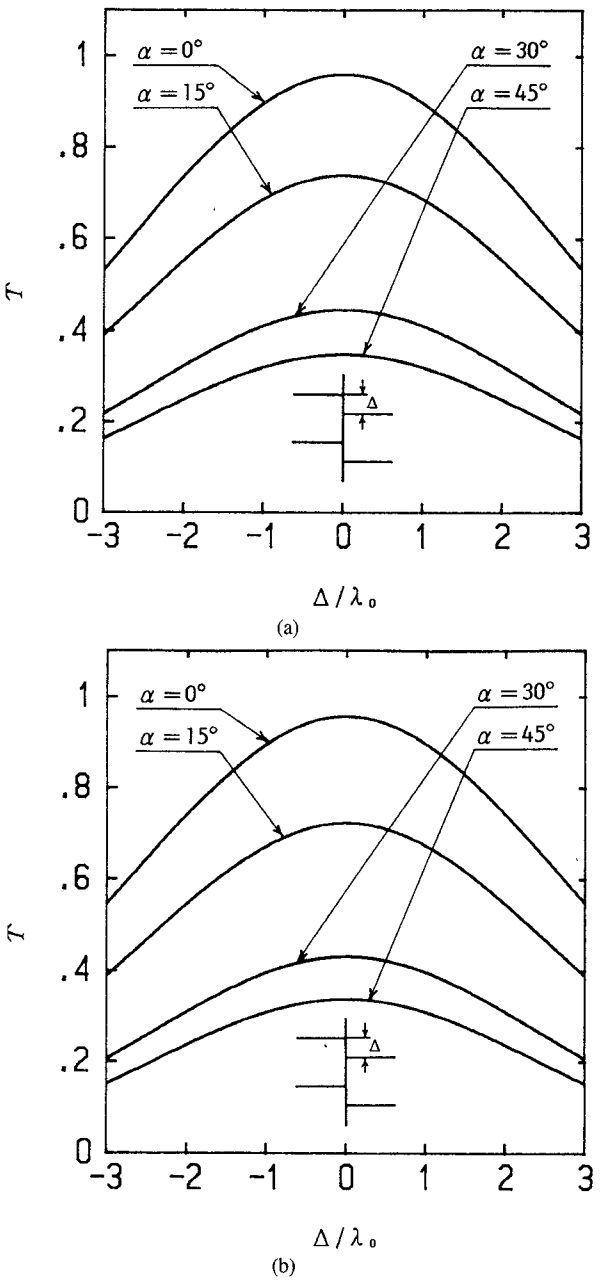

Fig. 2. Power-coupling coefficient versus normalized displacement distance with the oblique angle as a parameter. The outgoing waveguide has a symmetric structure: (a) step index profile and (b) square-law index profile. The structural parameters are chosen as $d_1 = d_2 = 5\lambda_0$, $n_{1c} = 1.51275$, $n_{1d} = 1.51$, $n_{od} = 2.272$, $n_{ed} = 2.187$, and $\delta n_o = \delta n_e = 0.002$.

The refractive indices are chosen as $n_{od} = (\epsilon_{od}/\epsilon_0)^{1/2} = 2.272$, $n_{ed} = (\epsilon_{ed}/\epsilon_0)^{1/2} = 2.187$, and $\delta n_o = \delta n_e = 0.002$ in the numerical calculations.

Fig. 2 shows curves for the power-coupling coefficients as a function of the normalized displacement distance Δ/λ_0 with the oblique angle α as a parameter. It is assumed in these cases that there is no angular misalignment between the two waveguide axes. Power coupling strongly depends on the oblique angle as well as the displacement distance whether the index profile of the waveguide 2 is graded or not.

The power-coupling coefficients are shown in Fig. 3 as a function of misalignment angle θ with the oblique angle

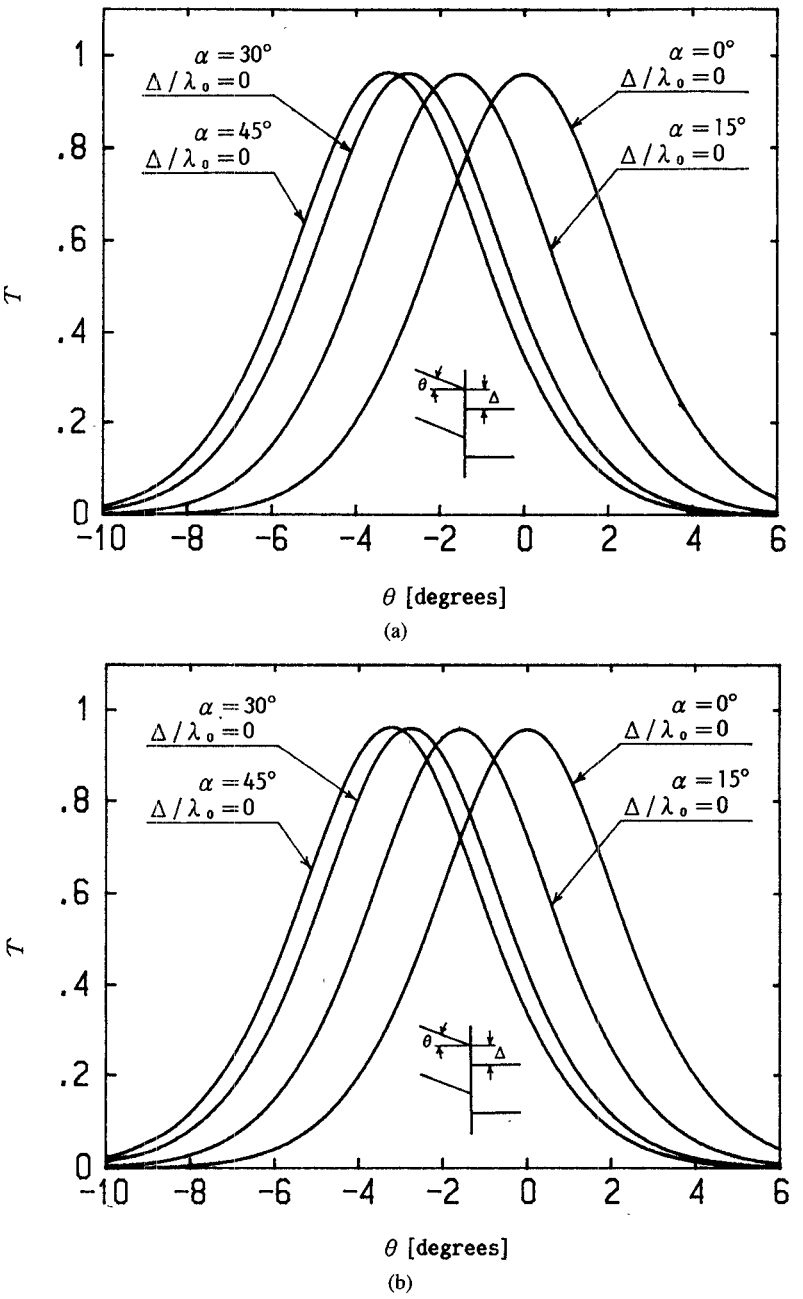

Fig. 3. Power-coupling coefficient versus misalignment angle with the oblique angle and the normalized displacement distance as parameters. The outgoing waveguide has a symmetric structure: (a) step index profile and (b) square-law index profile. The structural and material parameters are the same as in Fig. 2.

and the normalized displacement distance as parameters. The normalized Δ's in the figures are so optimally adjusted that the peak values become maximum. In these examples for the symmetric profiles, all of them are nearly equal to zero though. In the anisotropic waveguide, the misalignment in the waveguide and material coordinate systems causes the phase front to tilt in proportion to the oblique angle [12]. The values of θ at which the curves reach their peaks are almost identical to the tilt angles of phase fronts determined by the oblique angles written down in the figures. Consequently it is understood that close agreement of phase fronts in both incoming and outgoing waveguides is a principal factor for achieving high efficiency in power coupling at a butt-joint.

B. Asymmetric Index Profile

In general, index profiles are strongly asymmetric in practical waveguides by means of such usual fabrication techniques as diffusion processes or ion-exchange processes. We consider two representative index profiles also in this case. The first is a step-index profile

$$n_o(x) = \begin{cases} 1, & x < 0 \\ n_{od} + \delta n_o, & 0 \leqq x \leqq d_2 \\ n_{od}, & d_2 < x \end{cases}$$

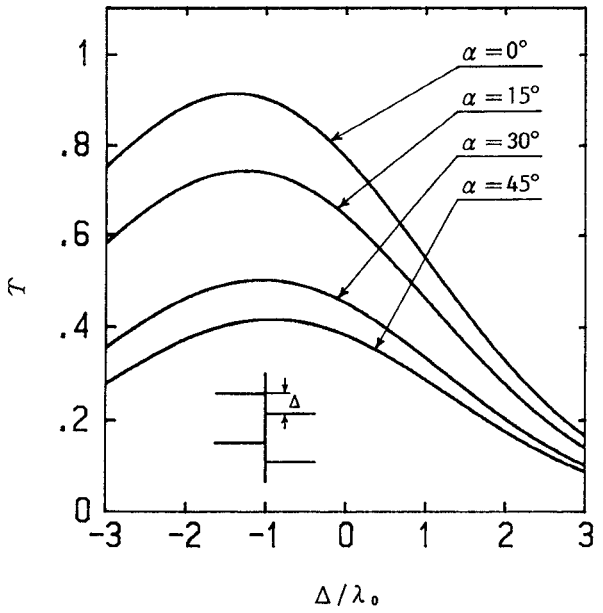

(a)

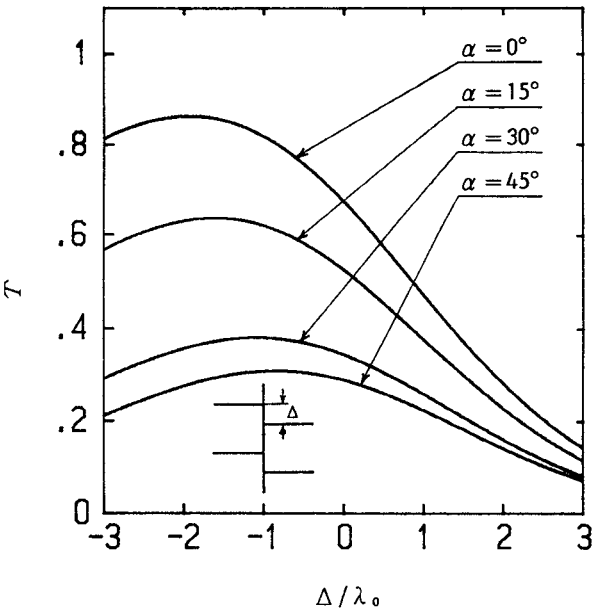

(b)

Fig. 4. Power-coupling coefficient versus normalized displacement distance with the oblique angle as a parameter. The outgoing waveguide has an asymmetric structure: (a) step index profile and (b) square-law index profile. The structural parameters are the same as in Fig. 2.

$$n_e(x) = \begin{cases} 1, & x < 0 \\ n_{ed} + \delta n_e, & 0 \leqq x \leqq d_2 \\ n_{ed}, & d_2 < x \end{cases} \tag{16}$$

and the second is a square-law index profile

$$n_o(x) = \begin{cases} 1, & x < 0 \\ n_{od} + \delta n_o[1 - (x/d_2)^2], & 0 \leqq x \leqq d_2 \\ n_{od}, & d_2 < x \end{cases}$$

$$n_e(x) = \begin{cases} 1, & x < 0 \\ n_{ed} + \delta n_e[1 - (x/d_2)^2], & 0 \leqq x \leqq d_2 \\ n_{ed}, & d_2 < x. \end{cases} \tag{17}$$

The refractive indices are chosen to be the same as before.

Fig. 4 illustrates the effects of axial displacement on the power-coupling coefficients. The abscissa represents the normalized displacement distance. The oblique angle is taken as a parameter. Each curve reaches its peak at

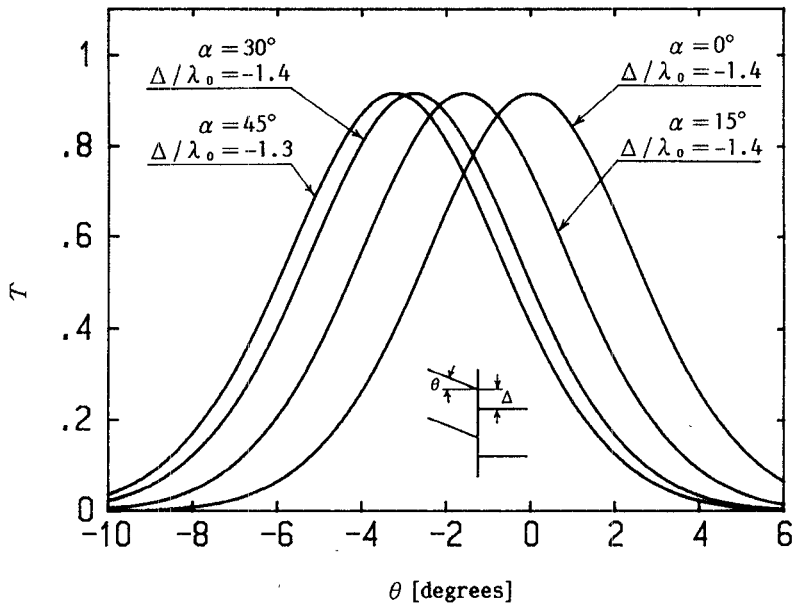

(a)

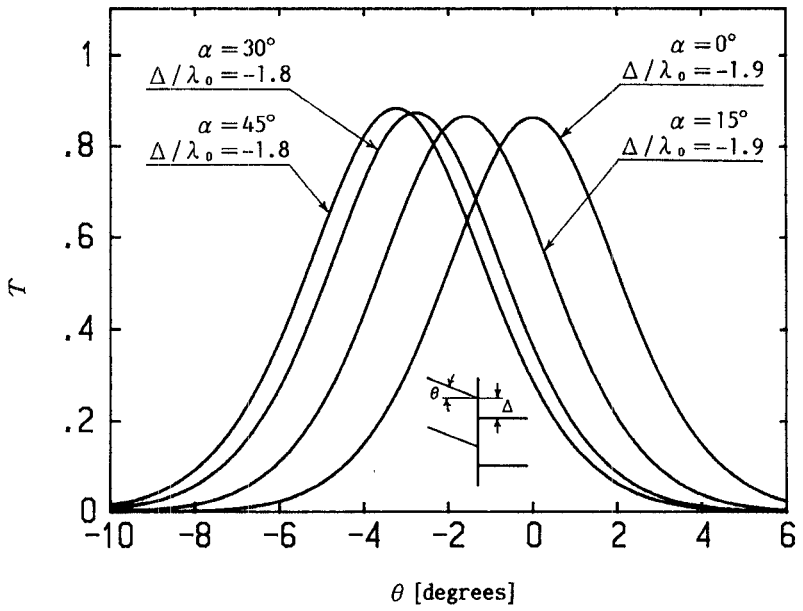

(b)

Fig. 5. Power-coupling coefficient versus misalignment angle with the oblique angle and the normalized displacement distance as parameters. The outgoing waveguide has an asymmetric structure: (a) step index profile and (b) square-law index profile. The structural and material parameters are the same as in Fig. 2.

other than $\Delta/\lambda_0 = 0$ because of asymmetry in the field profile caused by the asymmetric waveguide structure.

Finally, Fig. 5 shows curves for the power-coupling coefficients as a function of the misalignment angle with the oblique angle and the normalized displacement distance as parameters. Each one of normalized Δ's in the figures is optimally adjusted also in the present case. They are other than zero and slightly different from each other. An appropriate misalignment angle dramatically raises the efficiency of power coupling. Asymmetric index profiles support modes of asymmetric field profile, which must degrade the field overlapping between the two waveguide modes. This is the reason why each peak is a little bit lower than the corresponding peak of the former examples.

It is found from Figs. 4 and 5 that step index profiles show superior transmission characteristics to graded index profiles. A brief study on modal fields supported by asymmetric index profiles tells us that the field deformation from the symmetric case is more significant in graded index profiles; the spot-size is broader and the field distribution is less symmetric. Therefore, modal fields of step

index profiles match better with a symmetric field distribution of the incoming waveguide. This leads to the difference of the characteristics illustrated in the figures.

V. Conclusion

Power-coupling efficiency is analyzed for a butt-joint between an isotropic slab waveguide and an anisotropic one where the material coordinate system is not aligned with the waveguide coordinate system in the plane defined by the normal of waveguide surface and the propagation axis. The formula for power-coupling coefficients is derived from the boundary conditions at the interface between the incoming and outgoing waveguides by neglecting reflected radiation modes. A number of numerical results are presented for various values of the oblique angle, displacement distance, and misalignment angle. It is found that the misalignment of the material and waveguide coordinate systems in the anisotropic waveguide exceedingly lowers the power transmitted through the joint. It is also found that appropriate amounts of angular misalignment and axial displacement between the two waveguides improve power-coupling efficiency remarkably whether the index profile of outgoing waveguide is symmetric or not, and whether graded or not.

Appendix I

For the TM modes, the transverse magnetic field component of in the waveguide 1 is expressed as

$$H_{y'} = \begin{cases} A \exp(\gamma_1 x') \exp(-j\beta_1 z'), & x' < 0 \\ [A \cos(\kappa_1 x') + B \sin(\kappa_1 x')] \exp(-j\beta_1 z'), & 0 \leqq x' \leqq d_1 \\ [A \cos(\kappa_1 d_1) + B \sin(\kappa_1 d_1)] \cdot \exp[-\gamma_1(x' - d_1)] \exp(-j\beta_1 z'), & d_1 < x' \end{cases} \tag{A1}$$

where

$$\kappa_1 = [n_{1c}^2 k_0^2 - \beta_1^2]^{1/2}$$
$$\gamma_1 = [\beta_1^2 - n_{1d}^2 k_0^2]^{1/2}$$
$$k_0 = \omega(\epsilon_0 \mu_0)^{1/2} \tag{A2}$$
$$B = \frac{\gamma_1 n_{1c}^2}{\kappa_1 n_{1d}^2} A. \tag{A3}$$

"A" is an arbitrary constant and the eigenvalue equation is

$$\tan(\kappa_1 d_1) = \frac{2\kappa_1 \gamma_1 n_{1c}^2 n_{1d}^2}{\kappa_1^2 n_{1d}^4 - \gamma_1^2 n_{1c}^4}. \tag{A4}$$

With the help of the coordinate transformation

$$\begin{pmatrix} x \\ z \end{pmatrix} = \begin{pmatrix} \cos\theta & -\sin\theta \\ \sin\theta & \cos\theta \end{pmatrix} \begin{pmatrix} x' \\ z' \end{pmatrix} \tag{A5}$$

we obtain from (A1)

$$H_{y'} = \begin{cases} A \exp[\gamma_1(x \cos\theta + z \sin\theta)] \cdot \exp[-j\beta_1(-x \sin\theta + z \cos\theta)], & x < 0 \\ \{[A \cos[\kappa_1(x \cos\theta + z \sin\theta)] + B \sin[\kappa_1(x \cos\theta + z \sin\theta)]\} \cdot \exp[-j\beta_1(-x \sin\theta + z \cos\theta)], & 0 \leqq x \leqq d_1/\cos\theta \\ [A \cos(\kappa_1 d_1) + B \sin(\kappa_1 d_1)] \cdot \exp[-\gamma_1(x \cos\theta + z \sin\theta - d_1)] \cdot \exp[-j\beta_1(-x \sin\theta + z \cos\theta)], & d_1/\cos\theta < x. \end{cases} \tag{A6}$$

Finally, the relationships between the electric and magnetic fields

$$E_{x'} = \frac{j}{\omega\epsilon_{1p}} \frac{\partial H_{y'}}{\partial z'}$$
$$E_{z'} = \frac{-j}{\omega\epsilon_{1p}} \frac{\partial H_{y'}}{\partial x'} \tag{A7}$$

and the chain rule of differentiation lead to

$$E_{x'} = \frac{j}{\omega\epsilon_{1p}} \left(-\sin\theta \frac{\partial}{\partial x} + \cos\theta \frac{\partial}{\partial z}\right) H_{y'}$$
$$E_{z'} = \frac{-j}{\omega\epsilon_{1p}} \left(\cos\theta \frac{\partial}{\partial x} + \sin\theta \frac{\partial}{\partial z}\right) H_{y'}. \tag{A8}$$

Appendix II

$$h_1 = -2j \sin\theta \cos\theta \frac{\partial H_y^{(i)}}{\partial x} + j(\cos^2\theta - \sin^2\theta) \frac{\partial H_y^{(i)}}{\partial z}$$

$$= \begin{cases} A[\beta_1 \cos\theta - j\gamma_1 \sin\theta] \exp(\gamma_1 x \cos\theta) \cdot \exp(j\beta_1 x \sin\theta), & x < 0 \\ \{\beta_1 \cos\theta[A \cos(\kappa_1 x \cos\theta) + B \sin(\kappa_1 x \cos\theta)] - j\kappa_1 \sin\theta [-A \sin(\kappa_1 x \cos\theta) + B \cos(\kappa_1 x \cos\theta)]\} \exp(j\beta_1 x \sin\theta), & 0 \leqq x \leqq d_1/\cos\theta \\ [\beta_1 \cos\theta + j\gamma_1 \sin\theta][A \cos(\kappa_1 d_1) + B \sin(\kappa_1 d_1)] \exp[-\gamma_1(x \cos\theta - d_1)] \cdot \exp(j\beta_1 x \sin\theta), & d_1/\cos\theta < x \end{cases} \tag{A9}$$

$$h_2 = -2j \sin\theta \cos\theta \frac{\partial H_y^{(r)}}{\partial x} + j(\cos^2\theta - \sin^2\theta) \frac{\partial H_y^{(r)}}{\partial z}$$

$$= \begin{cases} -A[\beta_1 \cos\theta + j\gamma_1 \sin\theta] \exp(\gamma_1 x \cos\theta) \\ \quad \cdot \exp(-j\beta_1 x \sin\theta), \quad x < 0 \\ -\{\beta_1 \cos\theta[A \cos(\kappa_1 x \cos\theta) \\ \quad + B \sin(\kappa_1 x \cos\theta)] \\ \quad + j\kappa_1 \sin\theta [-A \sin(\kappa_1 x \cos\theta) \\ \quad + B \cos(\kappa_1 x \cos\theta)]\} \exp(-j\beta_1 x \sin\theta), \\ \quad 0 \leqq x \leqq d_1/\cos\theta \\ [-\beta_1 \cos\theta + j\gamma_1 \sin\theta][A \cos(\kappa_1 d_1) \\ \quad + B \sin(\kappa_1 d_1)] \exp[-\gamma_1(x \cos\theta - d_1)] \\ \quad \cdot \exp(-j\beta_1 x \sin\theta), \quad d_1/\cos\theta < x \end{cases} \tag{A10}$$

$$h_3 = j \frac{\partial H_y^{(t)}}{\partial x}. \tag{A11}$$

ACKNOWLEDGMENT

The authors wish to thank Dr. K. Yoshida, T. Sugawa, M. Nishie and S. Semura of the SUMITOMO Electric Industries, Ltd. for useful discussion and technical support of this work.

REFERENCES

[1] D. L. Bisbee, "Measurements of loss due to offsets and end separations of optical fibers," *Bell Syst. Tech. J.*, vol. 50, pp. 3159-3168, Dec. 1971.

[2] J. S. Cook, W. L. Mammel, and R. J. Grow, "Effect of misalignments on coupling efficiency of single-mode optical fiber butt joints," *Bell Syst. Tech. J.*, vol. 52, pp. 1439-1448, Oct. 1973.

[3] D. Gloge, "Offset and tilt losses in optical fiber splices," *Bell Syst. Tech. J.*, vol. 55, pp. 905-916, Sept. 1976.

[4] C. M. Miller, "Transmission vs transverse offset for parabolic-profile fiber splices with unequal core diameters," *Bell Syst. Tech. J.*, vol. 55, pp. 917-927, Sept. 1976.

[5] D. Marcuse, "Loss analysis of single-mode fiber splices," *Bell Syst. Tech. J.*, vol. 56, pp. 703-718, May-June 1977.

[6] L. G. Cohen, "Power coupling from GaAs injection lasers into optical fibers," *Bell Syst. Tech. J.*, vol. 51, pp. 573-594, Mar. 1972.

[7] T. C. Chu and A. R. McCormick, "Measurements of loss due to offset, end separation, and angular misalignment in graded index fibers excited by an incoherent source," *Bell Syst. Tech. J.*, vol. 57, pp. 595-602, Mar. 1978.

[8] J. M. Hammer and C. C. Neil, "Observations and theory of high-power butt coupling to $LiNbO_3$-type waveguides," *IEEE J. Quantum Electron.*, vol. QE-18, pp. 1751-1758, Oct. 1982.

[9] K. Morishita, S. Inagaki, and N. Kumagai, "Analysis of discontinuities in dielectric waveguides by means of the least squares boundary residual methods," *IEEE Trans. Microwave Theory Tech.*, vol. MTT-27, pp. 310-315, Apr. 1979.

[10] E. Nishimura, N. Morita, and N. Kumagai, "Theoretical investigation of a gap coupling of two dielectric slab waveguides with arbitrarily shaped ends," *Trans. IECE* (Japanese), vol. J67-C, pp. 714-721, Oct. 1984.

[11] T. Kambayashi and K. Hirai, "The reflection and transmission coefficients at the end of one rectangular dielectric waveguide connected to the other guide through a gap," *Trans. IEICE* (Japanese), vol. J72-C-I, pp. 271-273, Apr. 1989.

[12] D. Marcuse, "Modes of a symmetric slab optical waveguide in birefringent media—part I: optical axis not in plane of slab," *IEEE J. Quantum Electron.*, vol. QE-14, pp. 736-741, Oct. 1978.

[13] Y. Suematsu and K. Furuya, "Propagation mode and scattering loss of a two-dimensional dielectric waveguide with gradual distribution of refractive index," *IEEE Trans. Microwave Theory Tech.*, vol. MTT-20, pp. 524-531, Aug. 1972.

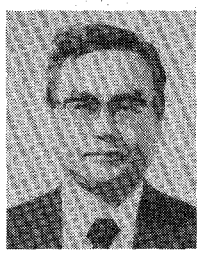

Shinnosuke Sawa (M'72) was born in Osaka, Japan, on October 23, 1938. He received the B.E. degree in electrical engineering from the University of Osaka Prefecture, Osaka, Japan, in 1962 and the M.E. and Ph.D. degrees in electrical communication engineering from Osaka University, Osaka, Japan, in 1967 and 1970, respectively.

From 1962 to 1964 he was with the Mitsubishi Electric Corporation, where he was engaged in ignitron manufacture and vacuum switch development at the corporation's Kyoto plant. From 1970 to 1991 he was with the Department of Electronics Engineering, Ehime University, Matsuyama, Japan. Since 1991 he has been a Professor in the Electrical Engineering Department, University of Osaka Prefecture, where his research has dealt with electronics theory, electromagnetic wave engineering, and optoelectronics. Currently, he is doing research on various waveguides from millimeter-wave through optical frequencies and on electromagnetic wave absorbers.

Dr. Sawa is a member of the Institute of Electronics, Information and Communication Engineers of Japan and the Institute of Electrical Engineers of Japan.

Masahiro Geshiro (S'75-M'78) received the B.E., M.E., and Ph.D. degrees in 1973, 1975, and 1978, respectively, from Osaka University, Osaka, Japan.

In December 1979 he joined the Department of Electronics, Ehime University, Matsuyama, Japan, where he is now an Associate Professor of Electronics Engineering. From March 1986 to January 1987, he was a Visiting Scholar at the University of Texas at Austin, on leave from Ehime University. He has been engaged in research on microwave and optical-wave transmission lines and integrated circuits.

Dr. Geshiro is a member of the Institute of Electronics, Information, and Communication Engineers of Japan.

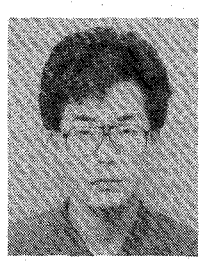

Masashi Hotta was born in Ehime, Japan, on August 19, 1965. He received the B.E. and M.E. degrees in electronics engineering from Ehime University, Ehime, Japan, in 1988 and 1990, respectively.

In April 1990 he joined the Department of Electronics, Ehime University, Matsuyama, Japan, where he is now an Assistant Professor of Electronics Engineering. He has been engaged in research and development of optoelectronics devices.

Mr. Hotta is a member of the Institute of Electronics, Information and Communication Engineers of Japan.

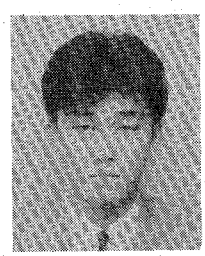

Haruo Kanetake was born in Ehime, Japan, on April 19, 1967. He received the B.E. degree in electronics engineering from Ehime University, Matsuyama, Japan, in 1990.

He is presently studying in the graduate school of electronics engineering, Ehime University, Matsuyama, Japan, where he has been engaged in research on coupling efficiency of optical waveguides.